

Received 16 May 2023, accepted 27 June 2023, date of publication 4 July 2023, date of current version 14 July 2023.

Digital Object Identifier 10.1109/ACCESS.2023.3292157

RESEARCH ARTICLE

Optical Parametric Oscillator Based on All-Optical Poled Silicon Nitride

SHIYI CHEN^{1,2}, MING YIN^{1,2}, YONGZHI LUO¹, AND XIYUE LIN¹

¹School of Mechanical and Electrical Engineering, Chengdu University of Technology, Chengdu 610059, China

²School of Industrial Technology, Chengdu University of Technology, Yibin 644000, China

Corresponding author: Ming Yin (yinming2014@cdu.edu.cn)

This work was supported in part by the Sichuan Science and Technology Program under Grant 2022NSFSC0901, in part by the Young and Middle-Aged Core Teacher Development Project of Chengdu University of Technology, and in part by the Higher Education Talent Training Quality and Teaching Reform Project of Chengdu University of Technology under Grant JG2130110.

ABSTRACT Quasi-phase matching optical parametric oscillators (OPOs) are widely used for mid-infrared laser generation. However, the traditional OPO bulk material using high voltage electric field poling limits the flexibility of the poling period. In this paper, we propose a novel OPO design based on all-optical poled silicon nitride, allowing for adjustable poling period. Two OPO design schemes are presented, each offering unique advantages in terms of operational characteristics and performance. The output characteristics of the OPO are investigated in three modes: OPO pump tuning, poling fundamental wave (PFW) tuning, and OPO pump tuning and PFW tuning with the same laser. For OPO pump tuning, the OPO achieves output wavelengths of 3.319-5.265 μm and 2.225-3.769 μm with PFW wavelengths of 1450 nm and 1700 nm. For PFW tuning, the OPO produces output wavelengths of 5.502-3.722 μm and 5.497-3.577 μm using OPO pump wavelengths of 1310 nm and 1654 nm, respectively. Furthermore, for OPO pump tuning and PFW tuning with the same laser, the OPO generates output wavelengths ranging from 5.504 μm to 3.941 μm with OPO pump and PFW wavelengths ranging from 1.420 μm to 1.610 μm . This new OPO design offers enhanced flexibility in controlling the poling period for efficient mid-infrared laser generation.


INDEX TERMS Optical parametric oscillator, periodically poled, silicon nitride, optical frequency conversion, infrared.

I. INTRODUCTION

Optical parametric oscillator (OPO) is widely used to generate mid-infrared lasers, to achieve differential absorption of substances or components, and for quantum communication [1], [2], [3].

In order to increase the coherence length in OPO and improve the efficiency of nonlinear frequency conversion, the interacting waves are usually required to meet the phase matching condition [4]. Phase matching generally includes birefringent phase matching (BPM) and quasi-phase matching (QPM). Compared to birefringent phase matching, QPM makes fuller use of the effective nonlinear coefficient of the nonlinear crystal, places less restriction on the poling state

of the wave, has no optical walk-off effect, etc. [5], [6], [7]. In order to achieve QPM, we often need to use periodic poling glasses, which are generally prepared by using a high voltage electric field poling method. However, the electric poling technique, which is currently the most widely used means of poling [8], [9], [10], [11], still has some limitations, such as the inability to modify the poling period again after setting up the OPO [12], and the experimental conditions are complex so we would prefer a simpler all-optical environment. It is worth noting that silicon nitride glasses can generate second-order nonlinearity by high-light irradiation. In addition, silicon nitride has a high Kerr nonlinear coefficient [13], wide transparency from the visible to the mid-infrared, a weak stimulated Brillouin scattering gain [14] and a low optical loss [15], [16]. Therefore, we propose an all-optical poling method to construct OPO utilizing

The associate editor coordinating the review of this manuscript and approving it for publication was Md. Selim Habib .

silicon nitride. We investigate the mechanism of second-order nonlinear coefficient generation in all-optical poled silicon nitride as an OPO bulk material, provide limits on the wavelength range of the poling fundamental wave (PFW), and calculate the tuning characteristics of the PFW to the poling period. Furthermore, we propose two OPO design schemes based on the environmental characteristics under all-optical poling and perform a quantitative analysis of the tuning of the OPO using PFW and OPO pump.

II. THEORETICAL ANALYSIS

A. SECOND-ORDER NONLINEARITY GENERATION

As an isotropic material, silicon nitride has a number of defects formed by Si-Si bonds which act as traps for electrons [17]. When irradiated by poling light, electrons in the center of the defects are excited, forming asymmetric photoelectron emission and inducing the coherent photoelectron effect [18], [19], [20]. Due to the quantum interference between multiphoton absorption processes in the two waves, electrons are emitted preferentially in space, resulting in photocurrent [17]:

$$j_{ph} = \beta E^2(\omega) E^*(2\omega) \exp(-i(k_{sh} - 2k_f)x) + c.c. \quad (1)$$

where β is the photogalvanic coefficient, $E(\omega)$ and $E^*(2\omega)$ are the local electric fields of the PFW and poling second harmonic wave (PSHW), respectively, k_f and k_{sh} are the wavevectors of the corresponding waves, and $c.c.$ is the complex conjugate.

The exponential term represents the coherent nature of the process and leads to a periodic separation of charges in space. As a result, charges migrate in a preferred direction, giving rise to a spatial DC electric field E_{DC} , as shown in (2). Finally, the $\chi^{(2)}$ grating, which is caused by mixing of third-order susceptibility and DC electric field, as shown in (3):

$$E_{DC} = -j_{ph}/\sigma \quad (2)$$

$$\chi^{(2)} = 3\chi^{(3)}E_{DC} \quad (3)$$

where σ is the photoconductivity, proportional to the total density of carriers promoted to the conduction band, $\chi^{(2)}$ is second-order susceptibility tensor, and $\chi^{(3)}$ is third-order susceptibility tensor.

According to (1), a three-photon absorption consisting of 2 PFW photons plus 1 PSHW photon generates some kind of spatial distribution related to phase matching ($k_{sh} - 2k_f$), and naturally the second harmonic generation process of all-optical poling is a QPM process. This automatic QPM allows for the conversion of optical parameters in a specific direction. At this point the poling period coincides with the spatial distribution pattern of the E_{DC} and is twice the coherence length of the PSHW and the PFW. This automatic QPM has been demonstrated by many studies [20], [21], [22], [23]. In addition, researchers have found that the poling period can be erased using high-energy photons, after which the material returns to isotropy and no longer has second-order nonlinearity [22].

B. SETTING OF THE PFW WAVELENGTH

The energy band gap of silicon nitride E is about 4.6 eV, and defects associated with Si-Si bonds act as electron traps within the band gap, with energy levels located above the valence band at 0.9-1.7 eV as the donor level E_1 , electron trap energy levels located 1.2-1.7 eV below the conduction band as the acceptor level E_2 . The energy difference between the donor level and acceptor level is ΔE [17]. Therefore, the electron from the center of the defect enters the conduction band in two steps: in the first step, the electron enters the acceptor level at an energy of just ΔE , which requires the absorption of 2 PFW photons or 1 PSHW photon; in the second step, the electron enters the conduction band from the acceptor level at an energy of more than E_2 , this process requires the absorption of a further 1 PSHW photon or 2 PFW photons.

Therefore ΔE needs to satisfy:

$$\Delta E = 2h\nu_f = 2hc/\lambda_f \quad (4)$$

where h is Planck's constant, c is the speed of light, and ν_f is the PFW frequency, and λ_f is the PFW wavelength.

Thus when ΔE satisfies condition (5), the silicon nitride can produce a nonlinear coefficient.

$$E_2 \leq \Delta E < 2E_2 \quad (5)$$

For the lower limit, since the 2 PFW photons and 1 PSHW photon have the same energy, the energy of the PFW (i.e., ΔE) should be no less than E_2 in the second step, allowing the electrons to enter the conduction band smoothly; for the upper limit, because the absorption of 1 PFW photon does not satisfy QPM ($k_{sh} - 2k_f$), and no second-order nonlinear coefficient can be generated. Therefore, E_2 must not be so small that the electrons can reach the conduction band after absorbing the energy of only 1 PFW photon (i.e., $1/2\Delta E$) in the second step and thus destroy the poling process.

Since the energy gap E and E_1 , E_2 , ΔE satisfy the relationship:

$$E_1 + E_2 + \Delta E = E \quad (6)$$

The wavelength range of the PFW λ_f can therefore be obtained from (4) (5) (6), as shown in Fig. 1.

$$\frac{3hc}{4.6 - E_1} < \lambda_f \leq \frac{4hc}{4.6 - E_1} \quad (7)$$

$$\frac{2hc}{3.4 - E_1} < \lambda_f \leq \frac{2hc}{2.9 - E_1} \quad (8)$$

As can be seen in Fig. 1, the upper limit of the PFW wavelength λ_f increases from 1.240 μm to 1.710 μm and the lower limit of the PFW wavelength λ_f increases from 1.005 μm to 1.459 μm in the silicon nitride transparent range as the donor level E_1 increases from 0.9 eV to 1.7 eV. Thus, when using all-optical poling, the PFW wavelength λ_f can be set at 1.005-1.710 μm .

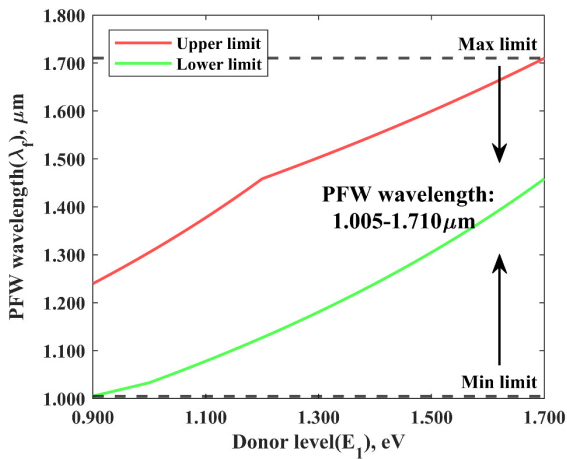


FIGURE 1. PFW wavelength λ_f as a function of donor level E_1 .

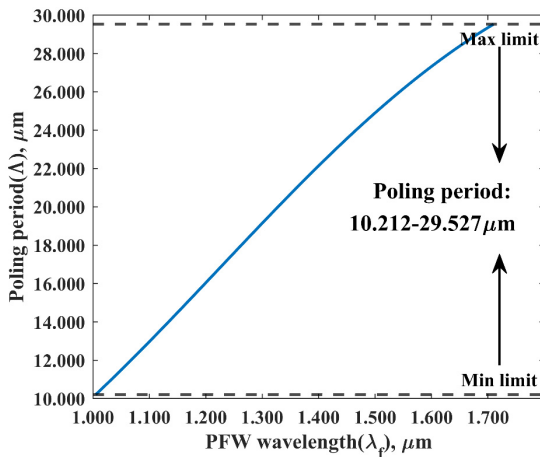


FIGURE 2. Variation of poling period Λ with PFW wavelength λ_f .

Based on the principle of QPM [24], the poling period Λ can be calculated:

$$\Lambda = \frac{\lambda_f}{2(n_{sh} - n_f)} \quad (9)$$

where n_f is the refractive index of PFW, and n_{sh} is the refractive index of PSHW.

The poling period Λ of silicon nitride varies with the PFW wavelength λ_f , as shown in Fig. 2. It can be seen that as the PFW wavelength λ_f increases from 1.005 μm to 1.710 μm , the poling period Λ increases from 10.212 μm to 29.527 μm .

It suggests that, compared to conventional periodic poling glasses, the poling period of silicon nitride can be tuned not only by conventional electrical poling methods, but also by the application of PFW, providing an alternative means of tuning the material.

III. RESULTS AND DISCUSSION

For conventional periodic poling glasses, the main ways of achieving the tuning of the output wavelength are: period tuning, angle tuning, temperature tuning, and tuning that changes

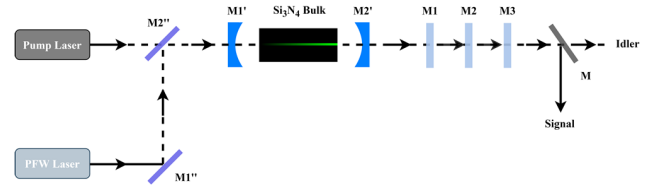


FIGURE 3. Diagram of all-optical poled OPO constructed using distinct lasers.

the wavelength of the pump. As silicon nitride glasses are subjected to all-optical poling, PFW can influence poling period, and then can affect the tuning of signal and idler. The gain of the OPO is derived from the interaction between waves, and the system should satisfy energy and momentum conservation [24]. Two equations are used to describe this process:

$$\frac{1}{\lambda_p} = \frac{1}{\lambda_s} + \frac{1}{\lambda_i} \quad (10)$$

$$\frac{2\pi n_p}{\lambda_p} - \frac{2\pi n_s}{\lambda_s} - \frac{2\pi n_i}{\lambda_i} - \frac{2\pi}{\Lambda} = 0 \quad (11)$$

where λ_p is the OPO pump wavelength, λ_s is the OPO signal wavelength, λ_i is the OPO idler wavelength, n_p is the OPO pump refractive index, n_s is the OPO signal refractive index and n_i is the OPO idler refractive index. The conversion efficiency of signal and idler is related to the length of the bulk material.

For OPO pump and PFW tuning, the OPO signal wavelength and the OPO idler wavelength can be calculated by coupling equations (9), (10) and (11).

In order to implement an all-optical OPO with silicon nitride bulk material, there are two ways to generate PFW and OPO pump: using a single laser or using two distinct lasers. To demonstrate the feasibility of these two approaches, we present the schematic diagrams for each case and provide a detailed analysis of the tuning characteristics for each method.

A. ALL-OPTICAL OPO CONSTRUCTED USING DISTINCT LASERS

When utilizing a bulk material of silicon nitride as the non-linear material in an all-optical OPO, where the PFW and OPO pump are generated by distinct lasers, the device configuration of the OPO is depicted in Fig. 3. The PFW laser emits PFW, which enters the silicon nitride through reflection mirrors $M1''$ and $M2''$. This causes the silicon nitride to generate a periodic second-order nonlinear coefficient. The pump laser emits OPO pump, which enters the OPO cavity and generates OPO signal and idler. The silicon nitride has OPO cavity mirrors $M1'$ and $M2'$ at both ends, which are coated with high-reflectivity coatings for the OPO signal and idler and high-transmittance coatings for the OPO pump, PFW, and PSHW. The OPO emits laser light, mainly comprising PFW, PSHW, OPO pump, OPO signal, and OPO idler. Filters $M1$, $M2$, and $M3$ can filter out PFW, PSHW, and OPO pump,

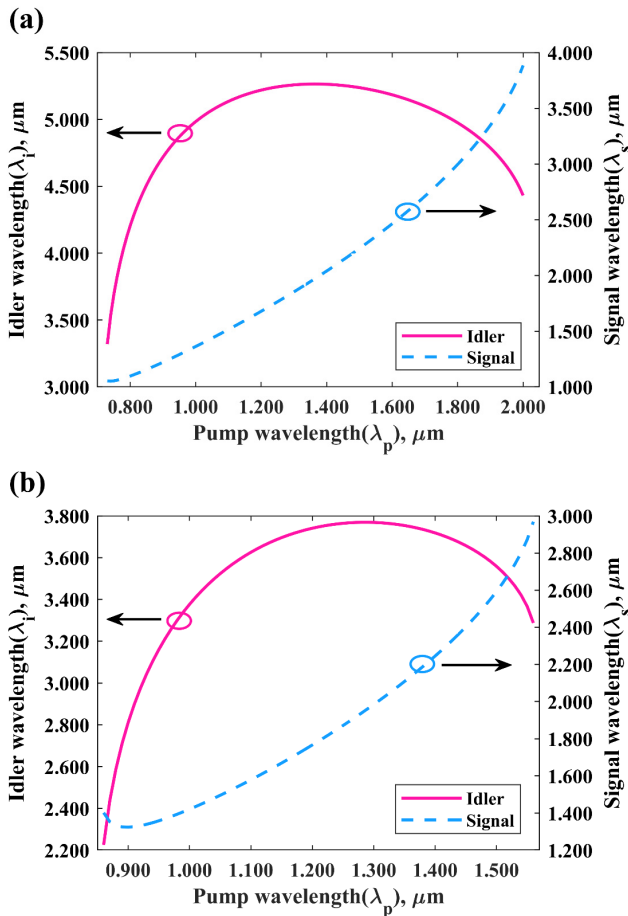


FIGURE 4. (a) Variation of OPO signal wavelength λ_s and idler wavelength λ_i with pump wavelength λ_p for a PFW wavelength λ_f of 1450 nm. (b) Variation of the OPO signal wavelength λ_s and the idler wavelength λ_i with the pump wavelength λ_p for a PFW wavelength λ_f of 1700 nm.

respectively. The beam splitter M separates the OPO signal and OPO idler.

In this case, the wavelength of the pump and the PFW are not related, and the wavelength can be set in a large range, which makes the tuning of OPO more flexible.

1) OPO PUMP TUNING

When the PFW wavelength λ_f is fixed, the OPO signal wavelength λ_s and the idler wavelength λ_i can vary with the pump wavelength λ_p . When the PFW wavelength λ_f is 1450 nm and 1700 nm, the OPO signal wavelength λ_s and the idler wavelength λ_i vary with the pump wavelength λ_p as shown in Fig. 4. When the PFW wavelength λ_f is 1450 nm, the OPO pump wavelength λ_p increases from 0.730 μm to 2.000 μm , the signal wavelength λ_s increases from 1.051 μm to 3.885 μm with a tuning width of 2.834 μm ; the idler wavelength λ_i increases from 3.319 μm to 5.265 μm and then decreases to 4.431 μm with a tuning width of 1.946 μm . When the PFW wavelength λ_f is 1700 nm, the OPO pump wavelength λ_p increases from 0.860 μm to 1.560 μm , the signal wavelength λ_s decreases from 1.402 μm to 1.324 μm and then increases

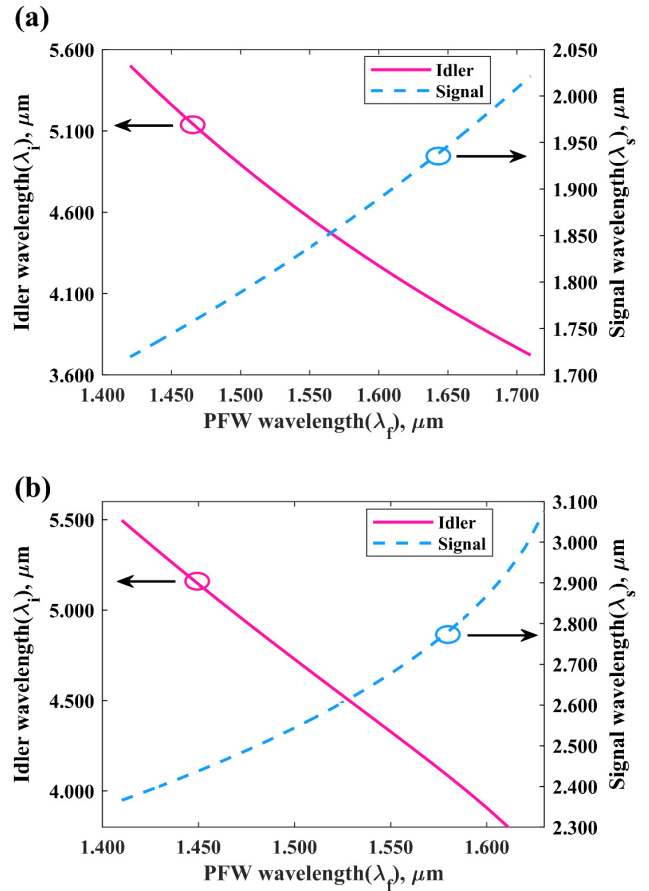


FIGURE 5. (a) Variation of OPO signal wavelength λ_s and idler wavelength λ_i with PFW wavelength λ_f for OPO pump wavelength λ_p of 1310 nm. (b) Variation of OPO signal wavelength λ_s and idler wavelength λ_i with PFW wavelength λ_f for an OPO pump wavelength λ_p of 1654 nm.

to 2.969 μm with a tuning width of 1.645 μm ; the idler wavelength λ_i increases from 2.225 μm to 3.769 μm and then decreases to 3.287 μm with a tuning width of 1.544 μm .

As can be seen from Fig. 4 (a) and (b), considering the transparent range of the silicon nitride and the fact that the calculation results will not be complex, it can be concluded that when the PFW wavelength λ_f is 1450 nm, the tunable range of pump wavelength (0.730 μm -2.000 μm) is larger than that when the PFW wavelength λ_f is 1700 nm (0.860 μm -1.560 μm), and accordingly, the tuning width of the signal and idler is somewhat larger, and the signal and idler wavelength does not necessarily vary monotonically.

2) PFW TUNING

When the OPO pump is fixed, the material poling period changes as the PFW wavelength λ_f changes, thus enabling the tuning of the OPO signal wavelength λ_s and the idler wavelength λ_i . When the OPO pump wavelength λ_p is 1310 nm and 1654 nm, the OPO signal wavelength λ_s and the idler wavelength λ_i change with the PFW wavelength λ_f as shown in Fig. 5. When the OPO pump wavelength λ_p is 1310 nm, the PFW wavelength λ_f changes from 1.420 μm to 1.710 μm ,

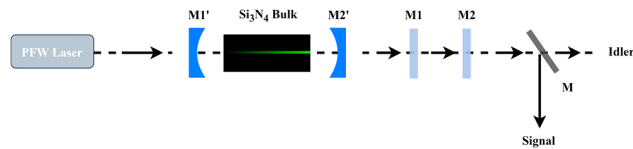


FIGURE 6. Diagram of all-optical poled OPO constructed using single laser.

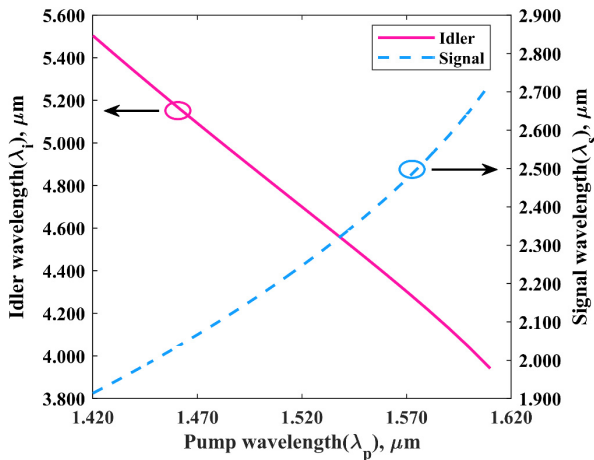


FIGURE 7. Variation of OPO signal λ_s and idler λ_i with OPO pump λ_p .

the signal wavelength λ_s changes from 1.719 μm to 2.022 μm with a tuning width of 0.303 μm ; the idler wavelength λ_i changes from 5.502 μm to 3.722 μm with a tuning width of 1.780 μm . When the OPO pump wavelength λ_p is 1654 nm, the PFW wavelength λ_f changes from 1.410 μm to 1.630 μm , the signal wavelength λ_s changes from 2.366 μm to 3.077 μm with a tuning width of 0.711 μm , and the idler wavelength λ_i changes from 5.497 μm to 3.577 μm with a tuning width of 1.920 μm .

As can be seen from Fig. 5 (a) and (b), as with the limits considered above for OPO pump tuning, when the OPO pump wavelength λ_p is 1310 nm, the tunable range of PFW wavelength (1.420 μm -1.710 μm) is larger than that when the OPO pump wavelength λ_p is 1654 nm (1.410 μm -1.630 μm), but it is worth noting that the tuning width of signal and idler is greater when tuning with 1654 nm OPO pump, and the wavelength of signal and idler varies monotonically.

B. ALL-OPTICAL OPO CONSTRUCTED USING SINGLE LASER

In an all-optical environment, we can simplify the OPO construction by using only one laser to generate PFW, which can both pole the silicon nitride and generate the OPO pump. The device configuration of the OPO is depicted in Fig. 6. The PFW laser emits PFW, which also serves as the OPO pump laser, generating OPO signal and idler when it enters the OPO cavity. This causes the silicon nitride to generate a periodic second-order nonlinear coefficient. The silicon nitride has OPO cavity mirrors M1' and M2' at both ends, which are coated with high-reflectivity coatings for the OPO signal and

idler and high-transmittance coatings for the OPO pump, PFW, and PSHW. The OPO output laser mainly includes PFW, PSHW, OPO pump, OPO signal, and OPO idler, among which the PFW and OPO pump have the same wavelength. Filters M1 and M2 can filter out the PFW/OPO pump and PSHW, respectively. The beam splitter M can separate the OPO signal and idler.

In this case, the wavelength of the pump is equal to the wavelength of the PFW, and the wavelength can be set in a smaller range, but the OPO device is simpler.

For device where the PFW and the OPO pump are generated by the same laser, the wavelength of the PFW is also the wavelength of the OPO pump. The wavelength of the OPO signal and the wavelength of the idler vary with the wavelength of the pump, as shown in Fig. 7.

As can be seen from Fig. 7, when the OPO pump wavelength λ_p changes from 1.420 μm to 1.610 μm , the signal wavelength λ_s changes from 1.914 μm to 2.722 μm with a tuning width of 0.808 μm ; the idler wavelength λ_i changes from 5.504 μm to 3.941 μm with a tuning width of 1.563 μm .

The device where the PFW and OPO pump are generated by same laser is simpler than the device where the PFW and OPO pump are generated by the distinct lasers, but then the tunable range of the pump is smaller. Among the three tuning modes, when the OPO pump is used, the tunable range and signal tuning width are the largest. There is little difference in the tuning width of idler among the three tuning modes.

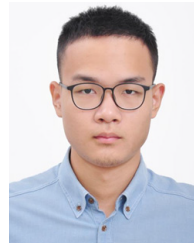
IV. CONCLUSION

In this paper, we investigate the utilization of silicon nitride for all-optical OPO. The PFW wavelength range, which can generate a periodic pattern, is found to be 1.005-1.710 μm . In the OPO pump tuning mode, we achieve output wavelengths of 3.319-5.265 μm and 2.225-3.769 μm by selecting PFW wavelengths of 1450 nm and 1700 nm. Similarly, in the PFW tuning mode, we obtain output wavelengths of 5.502-3.722 μm and 5.497-3.577 μm using OPO pump wavelengths of 1310 nm and 1654 nm. Additionally, when employing the single laser for both OPO pump and PFW tuning, we demonstrate output wavelength range of 5.504 μm to 3.941 μm with OPO pump and PFW wavelengths ranging from 1.420 μm to 1.610 μm . This paper highlights the versatility and tunability of the proposed all-optical OPO design, showcasing its potential for mid-infrared laser generation applications.

REFERENCES

- [1] J. Lu, A. Al Sayem, Z. Gong, J. B. Surya, C. Zou, and H. X. Tang, "Ultralow-threshold thin-film lithium niobate optical parametric oscillator," *Optica*, vol. 8, no. 4, pp. 539-544, 2021.
- [2] P. Parra-Rivas, L. Gelens, T. Hansson, S. Wabnitz, and F. Leo, "Frequency comb generation through the locking of domain walls in doubly resonant dispersive optical parametric oscillators," *Opt. Lett.*, vol. 44, no. 8, pp. 2004-2007, 2019.
- [3] E. Nitiss, J. Hu, A. Stroganov, and C.-S. Brès, "Optically reconfigurable quasi-phase-matching in silicon nitride microresonators," *Nature Photon.*, vol. 16, no. 2, pp. 134-141, Feb. 2022.

- [4] K. L. Vodopyanov, F. Ganikhanov, J. P. Maffettone, I. Zwieback, and W. Ruderman, "ZnGeP₂ optical parametric oscillator with 3.8–12.4- μ m tunability," *Opt. Lett.*, vol. 25, no. 11, pp. 841–843, 2000.
- [5] L. E. Myers, R. C. Eckardt, M. M. Fejer, R. L. Byer, W. R. Bosenberg, and J. W. Pierce, "Quasi-phase-matched optical parametric oscillators in bulk periodically poled LiNbO₃," *J. Opt. Soc. Amer. B, Opt. Phys.*, vol. 12, no. 11, pp. 2102–2116, 1995.
- [6] J. A. Armstrong, N. Bloembergen, J. Ducuing, and P. S. Pershan, "Interactions between light waves in a nonlinear dielectric," *Phys. Rev.*, vol. 127, no. 6, pp. 1918–1939, Sep. 1962.
- [7] H. Okayama, "Reduction of light signal pulse distortion in cascaded sum-frequency-generation and difference-frequency-generation wavelength conversion," *Opt. Rev.*, vol. 15, no. 5, pp. 236–240, Sep. 2008.
- [8] F. Ouellette, "Photosensitivity and self-organization in optical fibers and waveguides," *Proc. SPIE*, pp. 17–18, Aug. 1993.
- [9] P. G. Kazansky, A. Kamal, and P. S. J. Russell, "High second-order nonlinearities induced in lead silicate glass by electron-beam irradiation," *Opt. Lett.*, vol. 18, no. 9, pp. 693–695, 1993.
- [10] P. G. Kazansky, A. R. Smith, P. S. J. Russell, G. M. Yang, and G. M. Sessler, "Thermally poled silica glass: Laser induced pressure pulse probe of charge distribution," *Appl. Phys. Lett.*, vol. 68, no. 2, pp. 269–271, Jan. 1996.
- [11] X.-C. Long, R. A. Myers, and S. R. J. Brueck, "A poled electrooptic fiber," *IEEE Photon. Technol. Lett.*, vol. 8, no. 2, pp. 227–229, Feb. 1996.
- [12] P. G. Kazansky and P. S. J. Russell, "Thermally poled glass: frozen-in electric field or oriented dipoles," *Opt. Commun.*, vol. 110, nos. 5–6, pp. 611–614, Sep. 1994.
- [13] A. L. Gaeta, M. Lipson, and T. J. Kippenberg, "Photonic-chip-based frequency combs," *Nature Photon.*, vol. 13, no. 3, pp. 158–169, Mar. 2019.
- [14] F. Gyger, J. Liu, F. Yang, J. He, A. S. Raja, R. N. Wang, S. A. Bhave, T. J. Kippenberg, and L. Thévenaz, "Observation of stimulated Brillouin scattering in silicon nitride integrated waveguides," *Phys. Rev. Lett.*, vol. 124, no. 1, Jan. 2020, Art. no. 13902.
- [15] J. Liu, G. Huang, R. N. Wang, J. He, A. S. Raja, T. Liu, N. J. Engelsen, and T. J. Kippenberg, "High-yield, wafer-scale fabrication of ultralow-loss, dispersion-engineered silicon nitride photonic circuits," *Nature Commun.*, vol. 12, no. 1, pp. 1–9, Apr. 2021.
- [16] X. Ji, "Ultra-low-loss on-chip resonators with sub-milliwatt parametric oscillation threshold," *Optica*, vol. 4, no. 6, pp. 619–624, Jun. 2017.
- [17] A. Billat, D. Grassani, M. H. P. Pfeiffer, S. Kharitonov, T. J. Kippenberg, and C.-S. Brès, "Large second harmonic generation enhancement in Si₃N₄ waveguides by all-optically induced quasi-phase-matching," *Nature Commun.*, vol. 8, no. 1, pp. 1–7, Oct. 2017.
- [18] D. Z. A. Mizrahi and J. E. Sipe, "Model for second-harmonic generation in glass optical fibers based on asymmetric photoelectron emission from defect sites," *Opt. Lett.*, vol. 16, no. 11, pp. 796–798, 1991.
- [19] V. Mizrahi and J. E. Sipe, "Generation of permanent optically induced second-order nonlinearities in optical fibers by poling: Comment," *Appl. Opt.*, vol. 28, no. 11, p. 1976, 1989.
- [20] D. Grassani, M. H. Pfeiffer, T. J. Kippenberg, and C. Brès, "Second- and third-order nonlinear wavelength conversion in an all-optically poled Si₃N₄ waveguide," *Opt. Lett.*, vol. 44, no. 1, pp. 106–109, 2019.
- [21] E. Nitiss, O. Yakar, A. Stroganov, and C. Brès, "Highly tunable second-harmonic generation in all-optically poled silicon nitride waveguides," *Opt. Lett.*, vol. 45, no. 7, pp. 1958–1961, 2020.
- [22] E. Nitiss, T. Liu, D. Grassani, M. Pfeiffer, T. J. Kippenberg, and C. Brès, "Formation rules and dynamics of photoinduced X⁽²⁾ gratings in silicon nitride waveguides," *Acs Photon.*, vol. 7, no. 1, pp. 147–153, 2019.
- [23] J. Lin, N. Yao, Z. Hao, J. Zhang, W. Mao, M. Wang, W. Chu, R. Wu, Z. Fang, L. Qiao, W. Fang, F. Bo, and Y. Cheng, "Broadband quasi-phase-matched harmonic generation in an on-chip monocrystalline lithium niobate microdisk resonator," *Phys. Rev. Lett.*, vol. 122, no. 17, May 2019, Art. no. 173903.
- [24] E. G. Sauter, *Nonlinear Optics*. Hoboken, NJ, USA: Wiley, 1996, pp. 76–85.



SHIYI CHEN is currently working toward the B.S. degree with the School of Electrical Engineering, Chengdu University of Technology. His research interests include optoelectronic technology, FPGA design, and deep learning.

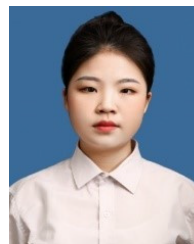


MING YIN received the B.S. degree in electronic science and technology and the Ph.D. degree in optical engineering from Sichuan University, Chengdu, China, in 2009 and 2014, respectively.

From 2014 to 2016, he was a Lecturer with the Electronic Information Engineering Department, Chengdu University of Technology, China. Since 2016, he has been an Associate Professor with the Electronic Information Engineering Department, Chengdu University of Technology. His research interests include optoelectronic technology, solid-state laser, and nonlinear optics. He is a Senior Member of the China Communication Society.



YONGZHI LUO received the B.S. degree from the School of Information Engineering, City College, Southwest University of Science and Technology, and the M.S. degree from the School of Mechanical and Electrical Engineering, Chengdu University of Technology. His research interests include laser transparent ceramics and optoelectronic technology.



XIYUE LIN received the B.S. degree from the School of Electrical Engineering, Chengdu Technological University, and the M.S. degree from the School of Mechanical and Electrical Engineering, Chengdu University of Technology. Her research interest includes optoelectronic technology.

...